Antifungal potency of terbinafine as a therapeutic agent against *Exophiala dermatitidis in vitro*

Tomofumi Nakamura[1,2†*], Tatsuya Yoshinouchi[1†], Mayu Okumura[2], Toshiro Yokoyama[3], Daisuke Mori[1], Hirotomo Nakata[2], Jun-ichirou Yasunaga[2], and Yasuhito Tanaka[1,4]

[1]Department of Laboratory Medicine, Kumamoto University Hospital, Kumamoto, Japan; [2]Department of Hematology, Rheumatology, and Infectious Diseases, Faculty of Life Sciences, Kumamoto University, Kumamoto, Japan; [3]Department of Medical Technology, Faculty of Health Science, Kumamoto Health Science University, Kumamoto, Japan; [4]Department of Gastroenterology and Hepatology, Faculty of Life Sciences, Kumamoto University, Kumamoto, Japan

† These authors contributed equally.

*To whom correspondence should be addressed; Tomofumi Nakamura, M.D., Ph.D.
E-Mail: tomona@kumamoto-u.ac.jp (T.N.); Tel: +81-096-373-5696; Fax: +81-096-373-5687.

Running title
Therapeutic potency of Terbinafine against Exophiala dermatitidis

Synopsis

Background: *Exophiala dermatitidis* (*E. dermatitidis*), which causes skin infections or respiratory diseases, is occasionally fatal in immunocompromised patients.

Objectives: Here, we report the unique antifungal potency of terbinafine (TRB), which targets squalene epoxidase, against *E. dermatitidis* ($SQLE^{ED}$) using various *in vitro* approaches.

Methods: Based on the human SQLE crystal structure, we created a structure model of $SQLE^{ED}$ using SWISS-MODEL and determined the best-fitting model of TRB to the $SQLE^{ED}$. The versatile antifungal activities, including fungicidal activity, biofilm inhibition, biofilm eradication activity, and the combination effect of TRB, posaconazole (PSC), and amphotericin B (AmB) with great antifungal potency against *E. dermatitidis* were evaluated using crystal violet and cell viability assay.

Results: Clinically isolated *E. dermatitidis* increased most vigorously at 30°C but decreased at 40°C. *E. dermatitidis* hyphae elongated and attached to a cell scaffold, forming a membrane-like biofilm that was distinct from the cell-free biofilm. In the binding model, TRB formed an H-bond with Y102 and was surrounded by key amino acid residues of $SQLE^{ED}$ corresponding to TRB-resistant mutations in *Trichophyton rubrum*, showing an

appropriate interaction. Among TRB, PSC, and AmB with potent antifungal activities, TRB and PSC showed more potent antibiofilm activities than AmB. In addition, TRB and PSC exhibited residual potency without incubation against *E. dermatitidis*, decreasing the growth at lower concentrations than AmB. In contrast, AmB exhibited strong time-dependent killing and eradication activities. The combination of TRB and PSC was more effective than that of TRB and AmB or PSC and AmB *in vitro*.

Conclusions: Although the tissue migration of TRB must be considered, these data suggest that TRB and PSC may be useful agents and a potent combination in severely immunocompromised patients with refractory and systemic *E. dermatitidis* infection.

Keywords: *Exophiala dermatitidis*, terbinafine, posaconazole, amphotericin B, biofilm

Introduction

It is estimated that 1.7 billion people worldwide suffer from fungal infections.[1] Invasive fungal infections in patients undergoing organ transplantation, chemotherapy for cancer, HIV infection, or autoimmune diseases cause approximately 1.7 million deaths per year.[2] *E. dermatitidis* is a black fungus, a member of the Herpotrichiellaceae, that can be isolated from wet living environments such as dishwashers, humidifiers, and bathtubs,[3] and is commonly reported as a pathogen of black fungal infections isolated from the skin and subcutaneous tissue in dermatological treatment.[4] Respiratory tract infections caused by *E. dermatitidis* are relatively rare, with reports of underlying diseases such as bronchiectasis and cystic fibrosis.[5,6] Moreover, black fungal infections caused by *E. dermatitidis* isolated from the skin, eye, liver, central nervous system, and central venous catheters have been reported as opportunistic fatal infections in immunocompromised patients.[7] *E. dermatitidis* has a slower growth rate than the other fungi. Small black colonies of *E. dermatitidis* observed on Sabouraud dextrose agar (SDA) after 3 days were barely detectable. Matrix-assisted laser desorption ionisation-time of flight mass spectrometry (MALDI-TOF MS) is a powerful tool for the early identification of pathogenic fungal species, including late-growing fungi such as *E. dermatitidis*, in addition to morphological and genetic analysis of the

specimen.[8] We previously reported *E. dermatitidis* pneumonia in immunocompromised patients with anorexia nervosa.[9] In clinical practice, *E. dermatitidis* is treated with azoles such as voriconazole and itraconazole for several months.[10,11] In this study, we analysed characteristics of *E. dermatitidis* and evaluated the antifungal, antibiofilm, killing (fungicidal) activity, and combinations of several clinically used oral and intravenous antifungal agents such as terbinafine (TRB)[13], azoles (fluconazole [FLC], miconazole [MCZ], voriconazole [VRC], itraconazole [ITC], PSC, isavuconazole [ISC]),[12] micafungin (MCF), caspofungin (CAS), and amphotericin B (AmB)[14] against *E. dermatitidis*. TRB, an allylamine medicine, showed a potent and unique anti-fungal effect against *E. dermatitidis*, which could lead to better treatment options that may prevent fatal *E. dermatitidis* infection in immunocompromised patients.

Material and Methods

Fungus and Cells

E. dermatitidis 1 and 2 isolated from the patients with pneumonia were identified by ESI-MS and ITS gene analysis[15], and *E. dermatitidis* 3 (NBRC6421, ATCC28869) was purchased from Biological Resource Center, NITE (NBRC, Japan) (Table S2). The fungus was incubated in Sabouraud buffer (5 g meat peptone, 5 g casein peptone, and 20 g glucose in 1L dH_2O) and Sabouraud dextrose agar (SDA) plate (5 g meat peptone, 5 g casein peptone, 40 g glucose, and 1.5% agar in 1L H_2O) supplemental with chloramphenicol (Cam) and kanamycin (K), or 0.25μm filtered RPMI (Nissui, Japan) without $NaHCO_3$ at pH 6.8, 0.165M 3-morpholinopropane-1-sulfonic acid, MOPS (MOPS-RPMI) supplemental with Cam and K. A549 cells isolated from a male patient with lung cancer were purchased from the Japanese Collection of Research Bioresources (JCRB) Cell Bank, Japan, and cultured in DMEM medium (FUJIFILM Wako Pure Chemical Corporation, Japan) supplemented with 10% fetal bovine serum (FBS; Gibco, Thermo Fisher Scientific, USA), penicillin (P), and K.

DNA and RNA extraction, and identification of SQLE sequences

A collection of *E. dermatitidis* incubated on SDA with a small medicine spoon was completely frozen in liquid nitrogen. After grinding with a masher tube, total RNA and DNA were extracted using TRIzole (Invitrogen, Thermo Fisher Scientific). RNA was converted into cDNA using ReverTra Ace® (TOYOBO, Japan). These primers (ITS4R: TCC TCC GCT TAT TGA TAT GC NS7F: GAG GCA ATA ACA GGT CTG TGA TGC) provided the best combination for identification with the strain of *E. dermatitidis* using the ITS sequence. PCR

amplifications were performed in an Eppendorf thermocycler (Eppendorf® Mastercycler) in a final volume of 40 μL with 10–50 ng of the DNA as a template using KOD one polymerase (TOYOBO). The SQLE amino acids sequence of *E. dermatitidis* was identified from the cDNA using these primers (ED.SE.SF: ATG CCT CTC ATA CTC GAT TCG TCG TC, ED.SE.ER: TCA AAT CCT CAG TTC GGC AAA TAT ATA CG, ED.SE.SQF: TCT GAT TCT GGG TGT GGA GTC C, ED.SE.SQR: TCA GGT ACG TCG ACC AGG ACA CG)

SQLE 3D structure and docking Simulation

The $SQLE^{ED}$ sequence was identified from the genomic DNA and RNA of *E. dermatitidis*. The 3D structure model of $SQLE^{ED}$ was produced as a template of the crystal structure of $SQLE^{Hum}$ (PDB accession number, 6C6N) using the SWISS model (https://swissmodel.expasy.org/). A nicotinamide adenine dinucleotide (NAD) was docked to the $SQLE^{ED}$ in the same manner as the crystal structure of $SQLE^{Hum}$ using SeeSAR v13.1 (BioSolveIT GmbH, Sankt Augustin, Germany).[48] Next, we determined the binding pocket of TRB using the 6C6N and clinically isolated TRB-resistant amino acid mutations of *T. rubrum* and performed the docking simulation of TRB to the $SQLE^{ED}$. Molecular graphics and analyses were performed using UCSF Chimera (https://www.rbvi.ucsf.edu/chimera).

Minimum Inhibitory Concentration

According to CLSI M38 3rd edition, *E. dermatitidis* was inoculated at 1.0×10^5 CFU/ml and incubated at 35°C for 48 or 72 hours in the flat-bottomed, 96-well plate with MOPS-RPMI. MIC (mg/L) represents the lowest concentration of antifungal agents that inhibited

the visible growth of *E. dermatitidis*. MIC_{50} and MIC_{90} (mg/L) are determined by measuring fungal growth at OD_{530} nm or proliferation of living cell at OD_{440} nm after staining 2-(4-Iodophenyl)-3-(4-nitrophenyl)-5-(2,4-disulfophenyl)-2H-tetrazolium, monosodium salt, WST-1 (Dojindo, Japan) using an absorbance spectrometer (FLUOstar Omega, BMG Labtech, Germany).

Drug combination

Drug combination assay referred to the previous report[25]. Briefly, combinations between TRB and azoles, AmB and azoles, TRB and AmB, or TRB and CAS at tested concentration were prepared in a polystyrene, flat-bottomed, 96-well plate with MOPS-RPMI medium. The conidium of *E. dermatitidis* was seeded at 1.0×10^5 CFU/mL and incubated at 35℃ for 48 or 72 hours. MIC (mg/L) was determined by the visible growth of *E. dermatitidis*. MIC_{50} and MIC_{90} (mg/L) were calculated by measuring fungal growth at OD_{530} nm or proliferation of living cells at OD_{440} nm after WST-1 staining. The FIC index (FICI) of tested combinations was identified according to previous reports[25,49]. Synergy effect decided FICI < 2.0, no interaction; 2.0 < FICI < 4.0, and antagonistic effect; FICI > 4.0. from each MIC, MIC_{50} (WST-1), and MIC_{90} (WST-1) data.

Time-kill assay

The time-kill assay of *E. dermatitidis* (1.0×10^6 CFU/ml) was performed in a microtube tube with 100 μL of MOPS-RPMI medium. TRB, AmB, and PCZ were tested at different concentrations ranging from 0.13 to 32 mg/L. The samples were shaken at 200 rpm, and

147 incubated at 35°C for 0, 3, 6, and 12 hours, respectively. The samples with or without drugs
148 at various concentrations were washed twice with 1000 μL phosphate-buffered saline (PBS)
149 at centrifugation of 2500 rpm for 2 minutes. The *E. dermatitidis* samples were duplicated
150 (final concentration, 2.5×10^5 CFU/ml) and inoculated into a 96-well plate with new 200 μL
151 of MOPS-RPMI medium without drugs at 35°C for 48 hours. The viable *E. dermatitidis* was
152 evaluated by the WST-1 staining assay.
153
154 **Observation of *E. dermatitis* morphology with or without A549 cells**
155 A549 cells were used to observe the adhesion ability of *E. dermatitis* by microscopy and
156 Scanning Electron Microscope (SEM), JSM-IT300 InTouchScope™.[9,50] A549 cells at $1.5 \times$
157 10^5/ml were inoculated into a 96-well plate or a coverslip, 18 × 18 mm, set on a chamber
158 slide II (IWAKI, Japan), filled with DMEM containing 10% FBS, P, and K. After O/N
159 incubation in 5% CO_2 at 37°C, the final concentration of *E. dermatitis* was added at 1.0×10^6
160 /mL to these plates, which were changed to DMEM containing 1% FBS, P, and K, and
161 incubated in 5% CO_2 at 35°C. The tested drugs at 0.25 mg/L were added to the plate after 6
162 hours. These samples were further incubated in 5% CO_2 at 35°C for 24 or 48 hours. The A549
163 cells and *E. dermatitis* in the 96-well plate were observed under a microscope after May-
164 Giemsa staining. The samples on the coverslip in the chamber slide II were fixed with 2%
165 glutaraldehyde in 0.1 M phosphate buffer (pH 7.4) for 24 or 48 hours and dehydrated through
166 50, 75, 90, 95, and 100% ethanol sequentially. The 100% ethanol was replaced with t-butyl
167 alcohol to cover the samples and stored at -20°C. The frozen sample was lyophilized under a
168 vacuum and was coated with platinum. SEM observation was performed.

169

170 **Biofilm Inhibition and Eradication**

171 Biofilm inhibition was determined using the crystal violet (CV) staining assay[23]. The
172 conidium of *E. dermatitidis* was seeded at 1.0×10^5 CFU/ml in a flat-bottomed, 96-well plate
173 with the tested drugs and incubated at 35℃ for 48 hours. The antifungal activity of the tested
174 drugs was also determined by measuring OD_{530}. The samples were washed twice with 200
175 μL PBS, and stained with 100 μL of a 0.1% CV solution for 20 minutes at room temperature.
176 The samples were washed again with 200 μL PBS and dried overnight. The 100 μL of 30%
177 acetic acid was incubated for 30 minutes to extract CV staining from the biofilm. The 80 μL
178 of the solution was transferred to a fresh 96-well plate and the samples were measured at
179 OD_{620} nm. Biofilm inhibition by the drugs was expressed as a relative ratio compared to
180 positive controls (no drugs). A modified biofilm eradication assay was performed according
181 to the previous report[51]. Briefly, the conidium of *E. dermatitidis* was seeded at 5.0×10^5
182 cells/ml in a 96-well plate without the tested drugs in 100 μL of MOPS-RPMI and incubated
183 at 35℃ for 24 hours. Then, the tested drugs were added to the plate at each concentration and
184 further incubated at 35℃ for 24 hours. The eradication ability of the tested drugs was
185 determined by the CV staining assay described above.

186

187 **Illustration**

188 Illustrations accompanying the experimental procedure and explanations were created
189 using BioRender: Scientific Image and Illustration Software.

190

191 **Drugs**

192 TRB, MCZ, VRC, ITC, and PSC were purchased from the Tokyo Chemical Industry Japan,
193 FLC and AmB from Wako Japan, ISC and CAS from Selleck Chemicals USA, and MCFG
194 from Cayman Chemical USA. These tested drugs (5–20 mM) in DMSO or appropriate
195 solutions were stored at -80℃. Before the assays, these drugs were prepared at appropriate
196 concentrations in MOPS-RPMI buffer.

197

198 # Results

199 ## Profile of clinically isolated *E. dermatitidis*

200 We observed giant black colonies of *E. dermatitidis* 1 isolated from a clinical patient[9]
201 under aerobic incubation at room temperature on SDA and performed morphological
202 observations using an optical microscope and scanning electron microscope (SEM) (Fig. 1).
203 The centre of the giant colonies formed a black gelatinous mass and the surface and edges
204 changed to olive brown (Fig. 1A). Microscopy revealed many yeast-like oval conidia in the
205 centre (Fig. 1B) and septate hyphae and hyphae in the outer part of the black colony (Fig.
206 1B). The internal transcribed spacer 1 (ITS1) and D1/D2 regions of the RNA were compared
207 using the Basic Local Alignment Search Tool (BLAST). The identification rate of the D1/D2
208 region was dominated by *Exophiala* species, and that of *E. dermatitidis* was 96.9%, and the
209 ITS region was 100% identical to *E. dermatitidis* (Fig. S1A). Based on genetic analysis of
210 the ITS region, we identified the giant black fungus as E. *dermatitidis* genotype A (Fig. S1B),
211 which is most commonly reported in Japan.[15]

212 Next, we analysed the growth of *E. dermatitidis* at 25, 30, 37, and 40℃. The growth
213 increased more efficiently at 30 and 37℃ than at 25 and 40℃ in MOPS-RPMI (Fig. 1C) and
214 Sabouraud medium (Fig. S1C). In addition, the diameter of the black colonies of *E.*

215 *dermatitidis* on SDA incubated for a week was 8.8, 8.0, 7.0, and 6.3 mm at 30, 37, 25, and
216 40°C, respectively, in line with the growth results at these temperatures (Fig. 1D). These
217 results suggest that the growth of *E. dermatitidis* was affected by incubation temperature; in
218 particular, incubation at 40°C prevented the growth. The benefit of thermotherapy in
219 cutaneous or subcutaneous infection has been previously reported.[16]
220
221 **Structural modelling of *E. dermatitidis* squalene epoxidase**
222 Target proteins of various antifungal drugs in clinical use are shown in Fig. 2. TRB target
223 squalene epoxidase (SQLE), also known as squalene monooxygenase, which catalyses the
224 conversion of squalene to (S)-2,3-epoxy squalene, is a key enzyme in ergosterol biosynthesis
225 in fungal membranes.[17,18] Azoles can also exert anti-fungal activity by inhibiting a different
226 target enzyme, lanosterol 14α-demethylase in the same pathway as shown in Fig. 2A.[19]
227 To investigate the structural antifungal efficacy of TRB against *E. dermatitidis*, we
228 identified the $SQLE^{ED}$ derived from three *E. dermatitidis* (Table S1) with the same amino
229 acid (AA) sequences. The AA sequences of SQLEs from humans, *E. dermatitidis*, and
230 *Trichophyton rubrum* were compared using Clustal omega (multiple sequence alignment
231 tool), as shown in Table S1. Moreover, the structural modelling of $SQLE^{ED}$ was produced by

SWISS-MODEL based on the crystallography of human SQLE ($SQLE^{Hum}$) (PDB:6C6N) as previously reported[18] and the full-length $SQLE^{Hum}$ model shown in Fig. 2B and S2A. Next, we performed a docking simulation of TRB to $SQLE^{ED}$ (Fig. 2B) based on the crystal structure of Cmpd-4 bound to $SQLE^{Hum}$ (PDB:6C6N) using SeeSAR (see Methods). The top 20 structures of the TRB bound to $SQLE^{ED}$ are shown in Fig. S2C. The TRB-binding structures of $SQLE^{Hum}$ and $SQLE^{ED}$ formed hydrogen bonds with the side chains of Tyr 122 and 102, respectively (Fig. S2). Important AA residues (L393, F397, F415, and H440) of SQLE ($SQLE^{TR}$) that bind to TRB have been reported in the resistance profiles of clinical isolates of *T. rubrum* (Fig. S2D).[31] TRB is surrounded by L410, F414, F432, and H459 of $SQLE^{ED}$, which correspond to L393, F397, F415, and H440 of $SQLE^{TR}$ in the biding respectively (Fig. 2C). These results indicate that TRB can effectively interact with $SQLE^{ED}$, resulting in a potent antifungal effect against *E. dermatitidis*.

Antifungal activity of clinically used drugs against *E. dermatitidis*

Various orally and intravenously administered antifungal drugs are available for clinical use. In this study, we evaluated the antifungal effects of ten drugs (FLC, MCZ, VRC, ITC, PCZ, ISC, TRB, AmB, CAS, and MCF) (Fig. S3) against clinically isolated *E. dermatitidis*

1 (Table 1) based on the CLSI-modified M38Ed3. Additionally, the susceptibilities of the other two *E. dermatitidis* strains (E.D.2, clinically isolated, and E.D.3, ATCC28869) to TRB, PSC, and AmB were evaluated (Table S2). The minimum inhibitory concentration (MIC), 50% inhibition of growth (MIC_{50}), and 90% inhibition of growth (MIC_{90}) were determined using $OD_{530,}$ or OD_{440} after WST-1 reagent staining to evaluate the viability of *E. dermatitidis* (WST-1 assay).[20] The MICs of FLC, MCF, and CAS against *E. dermatitidis* exceeded 16 mg/L as previously described.[21,22] PSC, VRC, AmB, TRB, and ITC showed potent inhibitory ability from 0.031 to 0.25 mg/L at MIC_{50} and MIC_{90} as assessed using OD_{530} and WST-1. MCZ at 0.25 to 0.5 mg/L inhibited the growth similarly to ISC. The MIC of these drugs was very close to MIC_{90} obtained from WST-1. *E. dermatitidis* exhibited different growth rates at different temperatures (Fig. 1C and S1C). To examine the effect of the incubation temperature on antifungal activity, we determined MIC_{50} and MIC_{90} of drugs by measuring *E. dermatitidis* growth at $OD_{530.}$ (Table S3). The findings indicated that incubation temperature did not significantly affect the antifungal activity of these drugs.

Inhibition and eradication of *E. dermatitidis*-induced biofilm

Bacterial and fungal biofilms form in infected organs, particularly on medical devices such

as intravascular catheters, artificial heart valves, and artificial joints, causing intractable chronic infections that are resistant to antibiotics and antifungals.[22] It has been reported that *E. dermatitidis* can produce biofilm formation.[23]

E. dermatitidis was incubated with or without A549 cells in a glass-bottomed slide chamber plate. *E. dermatitidis* without A549 cells floated in the buffer, whereas *E. dermatitidis* with A549 cells firmly attached to the bottom of the slide (Fig. S3). Next, we investigated the morphology of *E. dermatitidis* with or without A549 cells by optical microscopy (Fig. 3A) and SEM. (Fig. 3). The coadunate filamentous biofilm-like morphology of *E. dermatitidis* was sparsely observed without A549 cells as observed by SEM (Fig. S3). On the other hand, *E. dermatitidis* hyphae with the cells extended cohesively below and above the cells, and the oval conidia were diffusely attached to the cells for 24 hours of incubation (Fig. 3B). Moreover, membrane biofilm-like morphology including the cells appeared where *E. dermatitidis* was highly enriched for 48 hours of incubation (Fig. 3C and S3). Treatment with TRB, PSC, and AmB at 0.25 mg/L against *E. dermatitidis* inhibited hypha growth and showed pseudohyphae (Fig. 3D). There were no clear differences in *E. dermatitidis* morphology between these drug treatments.

Next, we examined the inhibitory and eradication abilities of TRB, PSC, and AmB against

283 *E. dermatitidis*-induced biofilms using a CV assay (Fig. 4 and S4). Interestingly, TRB and
284 PSC showed more potent inhibitory activity against the biofilm formation by *E. dermatitidis*
285 (Fig. 4B), and the antibiofilm activity of these drugs was similar to their anti-fungal activity
286 (Fig.S4). In contrast, AmB sufficiently and TRB slightly at high concentration eradicated the
287 *E. dermatitidis*-induced biofilm compared to PSC (Fig. 4C). These results indicate that TRB
288 and PSC can inhibit biofilm formation at lower concentrations than AmB. However, a higher
289 concentration of AmB can moderately eradicate the biofilm formed, suggesting that TRB and
290 PSC may be useful in the early treatment of acute *E. dermatitidis* infection and that AmB
291 may be effective in the late or prolonged treatment of chronic biofilm-forming infections.
292
293 **Fungicidal activity and combination effects of antifungal drugs against E. *dermatitidis***
294 The ability to kill invasive fungi is important in immunocompromised conditions.[24] We
295 examined a time course of the killing ability of these drugs using WST-1 reagent to examine
296 living *E. dermatitidis*. Notably, TRB, PSC, and AmB could be inhibited or killed by temporal
297 attachment (no incubation) to *E. dermatitidis* conidia (see Materials and Methods). (Fig. 5A
298 and B). TRB and PSC at lower concentrations (from 0.5 mg/L) decreased the growth of *E.*
299 *dermatitidis*, indicating that TRB and PSC rapidly interact with and maintain the target

300 proteins. In addition, during the observation of the killing ability of the drugs from 0 to 12
301 hours, TRB did not show any killing ability even at 32 mg/L. The viability of *E. dermatitidis*
302 incubated for 12 h at all TRB-tested concentrations increased compared to that without
303 incubation, suggesting that *E. dermatitidis* can withstand and show a reactive response to
304 TRB pressure (Fig. 5C). PSC and AmB killed *E. dermatitidis* in dose- and time-dependent
305 manner (Fig. 5D and E).

306 *In vitro* and *in vivo* combination therapies are effective in treating refractory and chronic
307 infections.[25] TRB and other antifungal combinations have been reported.[26] We investigated
308 the combinations of antifungal drugs such as TRB and azoles (PSC, VRC, and ITC), TRB
309 and AmB, and TRB and CAS against *E. dermatitidis* (Fig. 6 and S5). A previous study[21]
310 showed a synergistic effect against *E. dermatitidis* when CAS was combined with azoles
311 (VRC and ITC) *in vitro*. The fractional inhibitory concentration index (FICIs) was calculated
312 from the MIC, MIC_{50}, and MIC_{90} values in the WST-1 assay. The values for CAS and PCZ
313 were < 0.5, indicating a synergistic effect (Fig. S5). The value for the combination of TRB
314 and AmB was between 1.0 and 2.0, and that for PCZ and AmB between 1.0 and 2.2, resulting
315 in no interaction effects (Fig. 6). However, when a combination of TRB with other azoles
316 was examined, the FICI of TRB and PSC showed better efficacy between 0.31 and 0.75, TRB

317 and ISC between 0.63 and 1.0, TRB and ITC at 0.5, and TRB and VRC between 0.63 and
318 1.0, indicating synergistic or no interaction effects (Fig.6 and Fig. S5). These results suggest
319 that the combination of TRB with azoles that inhibit different target proteins in the same
320 pathway,[26] particularly ITC and PCZ, was more favourable than AmB against *E. dermatitidis*.
321 Taken together, TRB may be a therapeutic agent with novel antifungal, anti-biofilm, and
322 residual activities against *E. dermatitidis* in combination with azoles *in vitro* (Table 2).
323

Discussion

Systemic and invasive *E. dermatitidis* infections such as pneumonia and sepsis require a relatively long treatment period,[27] and have been reported to result in death.[8] Therefore, potent antifungal activity and tissue migration of antifungals to the site of infection are essential for antifungal treatment when treating immunocompromised patients.

In this study, TRB showed potent antifungal activity against *E. dermatitidis* similar to that of PSC in various *in vitro* assays. In addition, TRB showed a stronger anti-biofilm effect (Fig. 4A) than AmB, similar to PSC against fungus biofilm formation that is resistant even to disinfectants.[28] The residual potency of TRB for the treatment of *E. dermatitidis* does not require a higher effective drug concentration for a longer time (Fig. 4C), indicating that TRB exerts a dose- but not time-dependent effect on *E. dermatitidis* in terms of pharmacokinetic-pharmacodynamic parameters.[29]

TRB that targets SQLE is used in clinical practice as an oral medication, cream, and solution for the treatment of dermatomycoses such as *trichophytosis*.[30,31] The important AA residues (L393, F397, F415, and H440) of SQLE that bind to TRB have been reported in the resistance profiles of clinical isolates of *T. rubrum*.[32]

We identified the AA residues of $SQLE^{ED}$ from the genome and confirmed that the AA

residues at L410, F414, F432, and H459 of $SQLE^{ED}$ corresponded to those at L393, F397, F415, and H440 of $SQLE^{TR}$, respectively, indicating that there were no TRB resistance mutations against *E. dermatitidis* (Table S1 and S2). In the binding model, TRB formed an H-bond with Y102 and was surrounded by TRB resistance-related residues at L410, F414, F432, and H459, showing a better interaction (Fig.2 and Fig. S2). These data suggested that TRB can strongly bind to $SQLE^{ED}$, eliciting a potent antifungal effect.

TRB shows sufficient serum concentrations[33,34] and drug transfer to the skin and nails,[35] resulting in efficacy against dermatomycosis, but insufficient transfer to lung tissue[36,37] in animal models. Nevertheless, Oral administration of TRB has been reported to be effective in a few patients with chronic *Aspergillus* lung infections.[38,39] Clinical trials with larger numbers of patients are needed to evaluate the efficacy of TRB in the treatment of fungal pneumonia.

We believe that TRB prophylaxis or treatment of sepsis and infected sites with high blood flow may be effective, because TRB is a drug with sufficiently elevated blood levels, anti-biofilm, and potent residual effects. In contrast, direct administration of TRB as an external drug or by inhalation may be preferable in areas with poor blood flow and transitivity, such as intrabronchial fungal infections.

In this study, PSC showed a potent antifungal activity profile that was different from that of TRB against *E. dermatitidis*. According to a report on tissue concentrations in biopsy specimens obtained at autopsy from seven patients receiving PSC prophylaxis, lung concentrations were higher than those in the plasma.[40] The formulation of PSC is mixed with hydroxy-β-cyclodextrin, which improves its antifungal activity and pharmacokinetics by enhancing its solubility and oral bioavailability[41] as well as ITC.[42] These results suggest that PSC with improved tissue migration may be a suitable therapeutic option for invasive *E. dermatitidis* infections.

Recently, amikacin liposomal inhalation suspension (ALIS)[43] was developed for the treatment of refractory nontuberculous mycobacterial infectious pulmonary disease (NTM-PD) and demonstrated better efficacy in the CONVERT trial.[44] Direct administration at the site of infection, such as inhalation, can increase drug concentrations at the tissue level, resulting in greater antifungal efficacy than that of systemic administration, and leading to a reduction in the side effects of the drug. Inhalable and spray-dried microparticles of TRB[45,46] have been studied for the treatment of pulmonary fungal infections to enhance the beneficial effects of antifungal drugs as well as AmB.[47] TRB, which does not require particularly prolonged exposure (Fig. 4), would be a suitable inhaled drug for the treatment of *E.*

375 *dermatitidis* pneumonia, which has been reported in approximately 6 % of patients with
376 bronchiectasis and cystic fibrosis.[5] In addition, TRB may be a promising combination drug
377 (synergistic or indifferent effects *in vitro*) with azoles, including PSC, for the treatment of
378 invasive *E. dermatitidis* infections.

379 In conclusion, TRB could become an even more useful and attractive antifungal drug if new
380 routes of administration, such as inhalation or novel drug delivery systems, are developed to
381 enhance TRB tissue migration.

382

Acknowledgments

We thank the bacteriological examination staff of the Department of Laboratory Medicine at Kumamoto University Hospital.

Funding

This work was supported by the Japan Society for the Promotion of Science, KAKENHI grant number JP21K16324 (T.N.), and a grant from Kobayashi Foundation, Kobayashi pharmacy related grant (H.N.).

Transparency declarations

None to declare

Author contributions

T.N. and T.Y. designed the research and, T.N., T.Y., and M.O. performed all the experiments. T.Y., D.M., and H.N. discussed the data and supported the preparation of the research. Y.J. and Y.T. supervised the personnel and the study. T.N. and H.N. obtained the necessary funding. T.N. and T.Y. wrote the manuscript, and T.Y., D.M., Y.J., and Y.T. advised or edited

the manuscript. All authors read, commented on, and approved the final manuscript.

Supplementary data

Fig.S1 to S5 and Table S1 to S3 are available as Supplementary data at JAC Online.

References

1. Bongomin F, Gago S, Oladele RO *et al*. Global and Multi-National Prevalence of Fungal Diseases-Estimate Precision. J Fungi (Basel). 2017; **3**: 57. https://doi.org/10.3390/jof3040057.

2. Brown GD, Denning DW, Gow NA *et al*. Hidden killers: human fungal infections. Sci Transl Med. 2012; **4**: 165rv13. https://doi.org/10.1126/scitranslmed.3004404.

3. Döğen A, Kaplan E, Oksüz Z *et al*. Dishwashers are a major source of human opportunistic yeast-like fungi in indoor environments in Mersin, Turkey. Med Mycol. 2013; **51**: 493–8. https://doi.org/10.3109/13693786.2012.738313.

4. Isa-Isa R, García C, Isa M *et al.* Subcutaneous phaeohyphomycosis (mycotic cyst). Clin Dermatol. 2012; 30: 425–31. https://doi.org/10.1016/j.clindermatol.2011.09.015

5. Lebecque P, Leonard A, Huang D *et al.* Exophiala (Wangiella) dermatitidis and

417 cystic fibrosis Prevalence and risk factors. Med Mycol. 2010; **48**: S4–S9.
418 https://doi.org/10.3109/13693786.2010.495731

419 6. Vasquez A, Zavasky D, Chow NA *et al.* Management of an Outbreak of Exophiala
420 dermatitidis Bloodstream Infections at an Outpatient Oncology Clinic. Clin Infect Dis. 2018;
421 **66**: 959–62. https://doi.org/10.1093/cid/cix948.

422 7. Kirchhoff L, Olsowski M, Rath PM *et al.* Exophiala dermatitidis: Key issues of an
423 opportunistic fungal pathogen. Vol. 10, Virulence. Taylor and Francis Inc.; 2019; **10**: 984–
424 98. https://doi.org/10.1080/21505594.2019.1596504.

425 8. Kondori N, Erhard M, Welinder-Olsson C *et al.* Analyses of black fungi by matrix-
426 assisted laser desorption/ionization time-of-flight mass spectrometry (MALDI-TOF MS):
427 species-level identification of clinical isolates of Exophiala dermatitidis. FEMS Microbiol
428 Lett. 2015; **362**: 1–6. https://doi.org/10.1093/femsle/fnu016.

429 9. Yoshinouchi T, Yamamoto K, Migita M *et al.* Diagnosis and clinical management of
430 Exophiala dermatitidis pneumonia in a patient with anorexia nervosa: A case report. Med
431 Mycol Case Rep. 2023; **42**: 100617. https://doi.org/10.1016/j.mmcr.2023.100617.

432 10. Mpakosi A, Siopi M, Demetriou M *et al.* A fatal neonatal case of fungemia due to
433 Exophiala dermatitidis-case report and literature review. BMC Pediatr. 2022; **22**: 482.

https://doi.org/10.1186/s12887-022-03518-5.

11. Silva WC, Gonçalves SS, Santos DW *et al.* Species diversity, antifungal susceptibility and phenotypic and genotypic characterisation of Exophiala spp. infecting patients in different medical centres in Brazil. Mycoses. 2017; **60**: 328–37. https://doi.org/10.1111/myc.12597.

12. Shafiei M, Peyton L, Hashemzadeh M *et al.* History of the development of antifungal azoles: A review on structures, SAR, and mechanism of action. Bioorg Chem. 2020; **104**: 104240. https://doi.org/.1016/j.bioorg.2020.104240.

13. Petranyi G, Ryder NS, Stütz A. Allylamine derivatives: new class of synthetic antifungal agents inhibiting fungal squalene epoxidase. Science. 1984; **224**: 1239–41. https://doi.org/10.1126/science.6547247.

14. Brüggemann RJ, Jensen GM, Lass-Flörl C. Liposomal amphotericin B-the past. J Antimicrob Chemother. 2022; **77**: ii3–ii10. https://doi.org/10.1093/jac/dkac351.

15. Alimu Y, Ban S, Yaguchi T. Molecular Phylogenetic Study of Strains Morphologically Identified as Exophiala dermatitidis from Clinical and Environmental Specimens in Japan. Med Mycol J. 2022; **63**: 1–9. https://doi.org/10.3314/mmj.21-00012.

16. Naka W, Harada T, Nishikawa T. Growth Temperature of Pathogenic Dematiaceous

451 Fungi and Skin Surface Temperature. Jpn. J. Med. Mycol. 1986; **27**: 245–50,
452 https://doi.org/10.3314/JJMM1960.27.245

453 17. Petranyi G, Ryder NS, Stütz A. Allylamine derivatives: new class of synthetic
454 antifungal agents inhibiting fungal squalene epoxidase. Science. 1984; **224**: 1239–41.
455 https://doi.org/10.1126/science.6547247.

456 18. Padyana AK, Gross S, Jin L, Cianchetta G, *et al.* Structure and inhibition mechanism
457 of the catalytic domain of human squalene epoxidase. Nat Commun. 2019; **10**: 97.
458 https://doi.org/10.1038/s41467-018-07928-x.

459 19. Ghannoum MA, Rice LB. Antifungal agents: mode of action, mechanisms of
460 resistance, and correlation of these mechanisms with bacterial resistance. Clin Microbiol Rev.
461 1999; **12**: 501–17. https://doi.org/10.1128/CMR.12.4.501.

462 20. Ishiyama M, Miyazono Y, Sasamoto K, *et al.* A highly water-soluble disulfonated
463 tetrazolium salt as a chromogenic indicator for NADH as well as cell viability. Talanta. 1997;
464 **44**: 1299–305. https://doi.org/10.1016/s0039-9140(97)00017-9.

465 21. Sun Y, Liu W, Wan Z, Wang X *et al.* Antifungal activity of antifungal drugs, as well
466 as drug combinations against Exophiala dermatitidis. Mycopathologia. 2011; **171**: 111–7.
467 https://doi.org/10.1007/s11046-010-9358-6.

468 22. Sharma S, Mohler J, Mahajan SD *et al.* Microbial Biofilm: A Review on Formation,
469 Infection, Antibiotic Resistance, Control Measures, and Innovative Treatment.
470 Microorganisms. 2023; **11**: 1614. https://doi.org/10.3390/microorganisms11061614.
471 23. Kirchhoff L, Olsowski M, Zilmans K *et al.* Biofilm formation of the black yeast-
472 like fungus Exophiala dermatitidis and its susceptibility to antiinfective agents. Sci Rep.
473 2017; **7**: 42886. https://doi.org/10.1038/srep42886.
474 24. Pfaller MA, Sheehan DJ, Rex JH. Determination of fungicidal activities against
475 yeasts and molds: lessons learned from bactericidal testing and the need for standardization.
476 Clin Microbiol Rev. 2004; **17**: 268–80. https://doi.org/10.1128/CMR.17.2.268-80.2004.
477 25. Cuenca-Estrella M. Combinations of antifungal agents in therapy- what value are
478 they? J Antimicrob Chemother. 2004; **54**: 854–69. https://doi.org/10.1093/jac/dkh434.
479 26. Meletiadis J, Mouton JW, Meis JF *et al.* In vitro drug interaction modeling of
480 combinations of azoles with terbinafine against clinical Scedosporium prolificans isolates.
481 Antimicrob Agents Chemother. 2003; **47**: 106–17. https://doi.org/10.1128/AAC.47.1.106-
482 117.2003.
483 27. Lebecque P, Leonard A, Huang D *et al.* Exophiala (Wangiella) dermatitidis and
484 cystic fibrosis - Prevalence and risk factors. Med Mycol. 2010; **48**: S4-9.

https://doi.org/10.3109/13693786.2010.495731.

28. Sherry L, Ramage G, Kean R *et al.* Biofilm-Forming Capability of Highly Virulent, Multidrug-Resistant Candida auris. Emerg Infect Dis. 2017; **23**: 328–31. https://doi.org/10.3201/eid2302.161320.

29. Craig WA. Pharmacokinetic/pharmacodynamic parameters: rationale for antibacterial dosing of mice and men. Clin Infect Dis. 1998; **26**: 1–10. https://doi.org/10.1086/516284.

30. Sigurgeirsson B, Olafsson JH, Steinsson JB *et al.* Long-term effectiveness of treatment with terbinafine vs itraconazole in onychomycosis: a 5-year blinded prospective follow-up study. Arch Dermatol. 2002; **138**: 353–7. https://doi.org/10.1001/archderm.138.3.353.

31. Ramzi SHT, Arif SA, Majid A *et al.* Efficacy of Terbinafine and Itraconazole Combination Therapy Versus Terbinafine or Itraconazole Monotherapy in the Management of Fungal Diseases: A Systematic Review and Meta-Analysis. Cureus. 2023; **15**: e48819. https://doi.org/10.7759/cureus.48819.

32. Yamada T, Maeda M, Alshahni MM *et al.* Terbinafine Resistance of Trichophyton Clinical Isolates Caused by Specific Point Mutations in the Squalene Epoxidase Gene.

502 Antimicrob Agents Chemother. 2017; **61**: e00115–17. https://doi.org/10.1128/AAC.00115-
503 17.

504 33. Rojo-Solís C, García-Párraga D, Montesinos A *et al.* Pharmacokinetics of single
505 dose oral Terbinafine in common shelducks (Tadorna tadorna). J Vet Pharmacol Ther. 2021;
506 **44**: 510–15. https://doi.org/10.1111/jvp.12942.

507 34. Leyden J. Pharmacokinetics and pharmacology of terbinafine and itraconazole. J
508 Am Acad Dermatol. 1998; **38**: S42–7. https://doi.org/10.1016/s0190-9622(98)70483-9.

509 35. Faergemann J, Zehender H, Millerioux L. Levels of terbinafine in plasma, stratum
510 corneum, dermis-epidermis (without stratum corneum), sebum, hair and nails during and
511 after 250 mg terbinafine orally once daily for 7 and 14 days. Clin Exp Dermatol. 1994; **19**:
512 121–6. https://doi.org/10.1111/j.1365-2230.1994.tb01138.x.

513 36. Bechert U, Christensen JM, Poppenga R *et al.* Pharmacokinetics of terbinafine after
514 single oral dose administration in red-tailed hawks (Buteo jamaicensis). J Avian Med Surg.
515 2010; **24**: 122–30. https://doi.org/10.1647/2008-052.1.

516 37. Schmitt HJ, Andrade J, Edwards F *et al.* Inactivity of terbinafine in a rat model of
517 pulmonary aspergillosis. Eur J Clin Microbiol Infect Dis. 1990; **9**: 832–5.
518 https://doi.org/10.1007/BF01967386.

519 38. Schiraldi GF, Lo Cicero G, Rossetti C *et al.* Terbinafine versus itraconazole: a long-
520 term, randomized, double-blind, clinical trial in chronic pulmonary aspergillosis. A pilote
521 study. Journal of Health and Social Sciences. 2016; **1**: 47–56.
522 https://doi.org/10.1910.19204/2016/trbn7.

523 39. Schiraldi GF, Cicero SL, Colombo MD *et al.* Refractory pulmonary aspergillosis:
524 compassionate trial with terbinafine. Br J Dermatol. 1996; **134**: 25–9: discussion 39-40.
525 https://doi.org/10.1111/j.1365-2133.1996.tb15656.x.

526 40. Blennow O, Eliasson E, Pettersson T *et al.* Posaconazole concentrations in human
527 tissues after allogeneic stem cell transplantation. Antimicrob Agents Chemother. 2014; **58**:
528 4941–3. https://doi.org/10.1128/AAC.03252-14.

529 41. Greer ND. Posaconazole (Noxafil): a new triazole antifungal agent. Proc (Bayl Univ
530 Med Cent). 2007; **20**: 188–96. https://doi.org/10.1080/08998280.2007.11928283.

531 42. Mouton JW, van Peer A, de Beule K *et al.* Pharmacokinetics of itraconazole and
532 hydroxyitraconazole in healthy subjects after single and multiple doses of a novel
533 formulation. Antimicrob Agents Chemother. 2006; **50**: 4096–102.
534 https://doi.org/10.1128/AAC.00630-06.

535 43. Zhang J, Leifer F, Rose S, Chun DY *et al.* Amikacin Liposome Inhalation

536 Suspension (ALIS) Penetrates Non-tuberculous Mycobacterial Biofilms and Enhances
537 Amikacin Uptake Into Macrophages. Front Microbiol. 2018; **9**: 915.
538 https://doi.org/10.3389/fmicb.2018.00915.

539 44. Griffith DE, Eagle G, Thomson R *et al.* Winthrop KL; CONVERT Study Group.
540 Amikacin Liposome Inhalation Suspension for Treatment-Refractory Lung Disease Caused
541 by Mycobacterium avium Complex (CONVERT). A Prospective, Open-Label, Randomized
542 Study. Am J Respir Crit Care Med. 2018; **198**: 1559–69.
543 https://doi.org/10.1164/rccm.201807-1318OC.

544 45. Almansour K, Alfagih IM, Aodah AH *et al.* Inhalable, Spray-Dried Terbinafine
545 Microparticles for Management of Pulmonary Fungal Infections: Optimization of the
546 Excipient Composition and Selection of an Inhalation Device. Pharmaceutics. 2021; **14**: 87.
547 https://doi.org/10.3390/pharmaceutics14010087.

548 46. Brunet K, Martellosio JP, Tewes F *et al.* Inhaled Antifungal Agents for Treatment
549 and Prophylaxis of Bronchopulmonary Invasive Mold Infections. Pharmaceutics. 2022; **14**:
550 641. https://doi.org/10.3390/pharmaceutics14030641.

551 47. de Pablo E, O'Connell P, Fernández-García *et al.* Targeting lung macrophages for
552 fungal and parasitic pulmonary infections with innovative amphotericin B dry powder

553 inhalers. Int J Pharm. 2023; **635**: 122788. https://doi.org/10.1016/j.ijpharm.2023.122788.

554 48. Nakamura T, Okumura M, Takamune *et al.* Conversion of raltegravir carrying a

555 1,3,4-oxadiazole ring to a hydrolysis product upon pH changes decreases its antiviral activity.

556 PNAS Nexus. 2023; **3**: pgad446. https://doi.org/10.1093/pnasnexus/pgad446.

557 49. Odds FC. Synergy, antagonism, and what the chequerboard puts between them. J

558 Antimicrob Chemother. 2003; **52**: 1. https://doi.org/10.1093/jac/dkg301.

559 50. Ichikawa T, Kutsumi Y, Sadanaga J *et al.* Adherence and Cytotoxicity of Candida

560 spp. to HaCaT and A549 cells. Med Mycol J. 2019; **60**: 5–10.

561 https://doi.org/10.3314/mmj.18-00011.

562 51. Pierce CG, Uppuluri P, Tristan AR *et al.* A simple and reproducible 96-well plate-

563 based method for the formation of fungal biofilms and its application to antifungal

564 susceptibility testing. Nat Protoc. 2008; **3**: 1494–500. https://doi.org/10.1038/nport.2008.141.

565

Figure legends

Figure 1 Characteristics of *E. dermatitidis*

A) *E. dermatitidis* colony incubated on an SDA plate for 14 days was black gelatinous in the centre, changing to brown at the edges. The lactophenol cotton blue-stained specimen image was observed by the slide culture method. **B**) Morphological image of the central and marginal areas of *E. dermatitidis* colony by SEM. The scale bar and magnification at each image are shown **C**) Growth rate and microscopic images of *E. dermatitidis* in MOPS-RPMI culture medium until 108 hours or **D**) colonies on the SDA plate for 120 hours at 25, 30, 37, and 40℃, respectively.

Figure 2 Targets of antifungal drugs and SQLE structures

A) Schematic illustration of antifungal target proteins in fungal cells. **B**) The best binding model of TRB to the SQLE structure of *E. dermatitidis* with nicotinamide adenine dinucleotide (NAD). TRB interacts with Y102 through an H-bond in $SQLE^{ED}$. **C**) The location of putative TRB-resistant amino acid residues (L410, F414, F432, and H459) in the $SQLE^{ED}$ structure corresponding to clinically TRB-resistant mutations (L393F/S, F397L, F415L/I/V, and H440Y) in the $SQLE^{TR}$.

Figure 3 Morphology of *E. dermatitidis* with A549 cells

A) May-Giemsa staining on A549 cells. *E. dermatitidis* was observed by optical microscopy incubated at 35℃ for 24 hours after addition to the A549 cells. **B**) *E. dermatitidis* hyphae

were elongated and attached to the 549 cells incubated at 35℃ for 24 hours by SEM. **C**) Gray-membrane biofilm containing A549 cells circled at the dotted yellow line formed on enriched *E. dermatitidis* after incubation at 35℃ for 48 hours. **D**) *E. dermatitidis* incubated on the A549 cells at 35℃ for 24 hours in the presence of TRB, AmB, and PSC at 0.25 mg/L. The scale bar and magnification at each image are shown in white.

Figure 4 Inhibition and eradication of biofilm activity of TRB, PSC, and AmB

A) Schematic illustration shows assay procedures to confirm inhibition and eradication of TRB, PSC, and AmB against *E. dermatitidis* biofilm. **B**) Biofilm inhibition and **C**) eradication potency of TRB (green circle), PSC (blue triangle), and AmB (yellow square) are shown as a relative ratio (positive control is no drug) from 0.078 to 1 mg/L and from 0.063 to 16 mg/L, respectively. All assays were performed independently in triplicate. Means (± S.D.) of all data are presented.

Figure 5 Residual and killing activity of TRB, PSC, and AmB

A) Schematic illustration of assay procedures to confirm the residual and killing potency of TRB, PSC, and AmB against *E. dermatitidis*. **B**) Residual potency of TRB (green circle), PSC (blue triangle), AmB (yellow square), and CAS (purple × mark) treated with no incubation time (0 h) is shown as a relative ratio (positive control is no drug) from 0.125 to 32 mg/L. Assays were performed independently in triplicate. Means (± S.D.) of all data are

608 presented. The killing potency of **C**) TRB, **D**) PSC, and **E**) AmB were evaluated and shown
609 as relative ratios at each appropriate concentration and incubation time as assessed by cell
610 viability using WST-1 staining. Assays were performed independently in triplicate. Means (±
611 S.D.) of representative data are shown.
612

613 **Figure 6 Combination effect of TRB, PSC, and AmB on *E. dermatitidis***

614 A combination of **A**) TRB and PSC, **B**) TRB and AmB, and **C**) AmB and PSC tables and 3D
615 surface plots consist of relative ratios at each appropriate concentration as assessed by *E.*
616 *dermatitidis* viability using WST-1 staining. FIC indices (FICI) were evaluated as synergy;
617 FICI < 0.5, no interaction; 0.5 < FICI < 4, or antagonism; FICI > 4, which calculated from
618 MIC (*in red) data or MIC_{50} (***) and MIC_{90} (**) of WST-1 staining results. All assays were
619 performed independently in triplicate and representative data are shown.

Figure.1

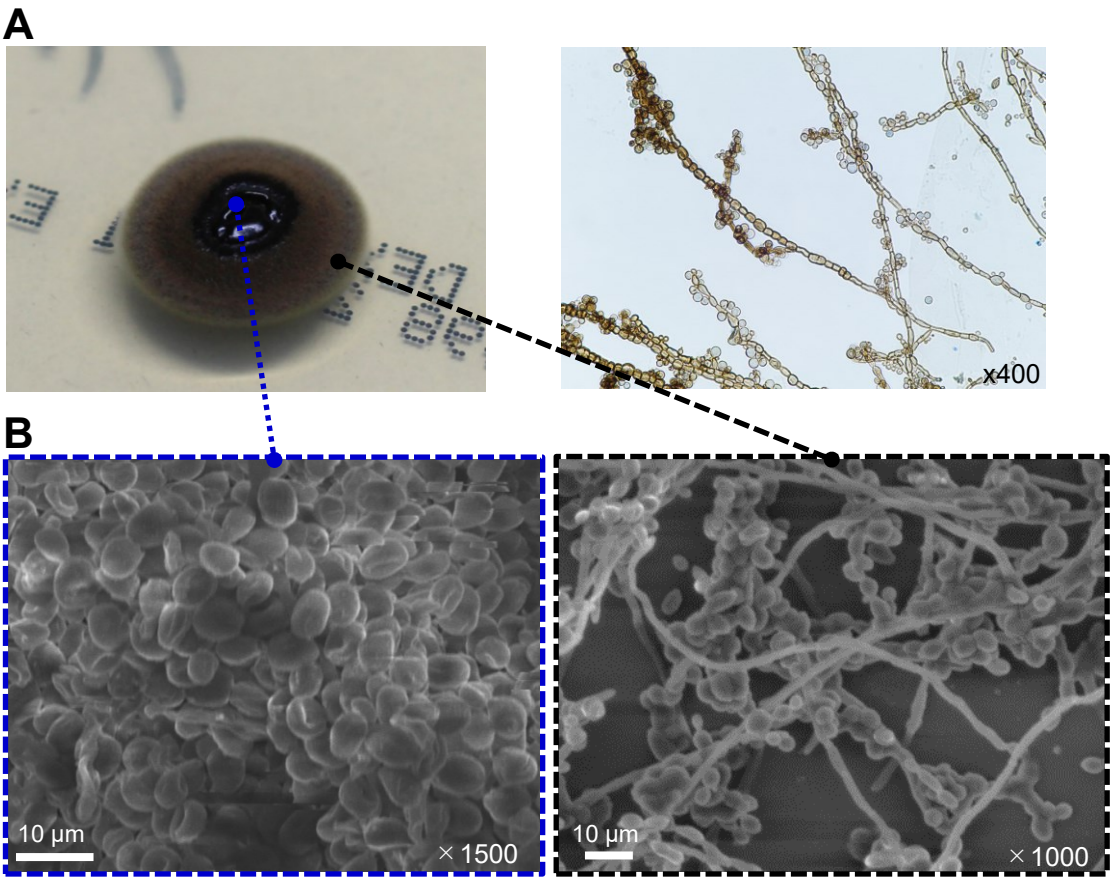

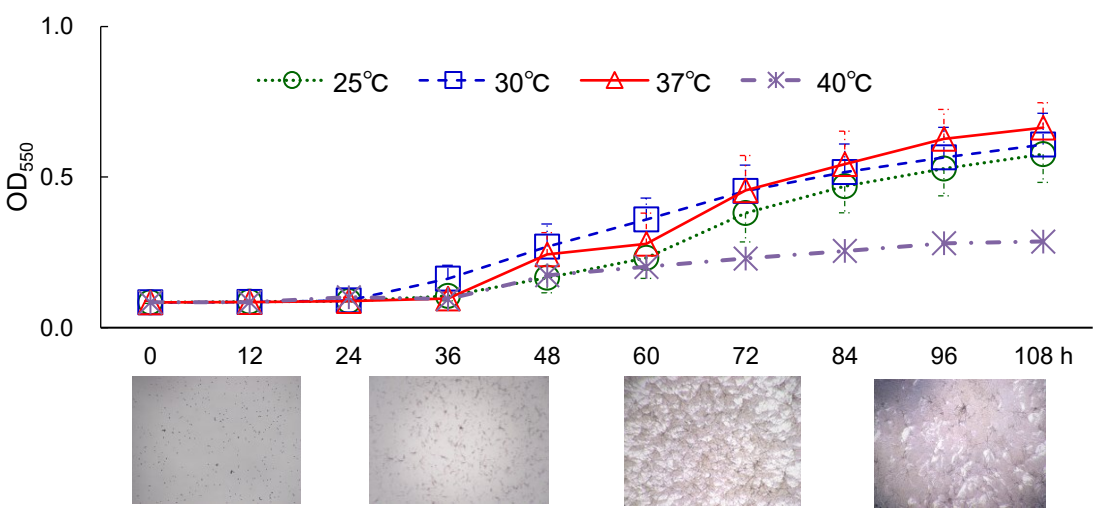

D

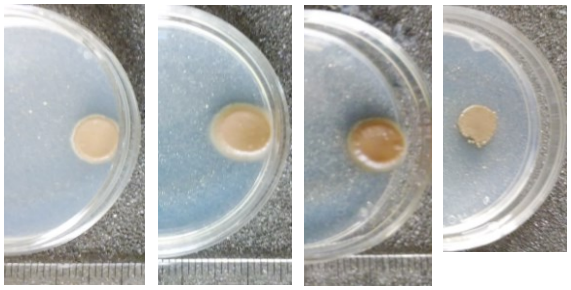

Day 5 (mm)	25℃	30℃	37℃	40℃
Φ fungal colony	7.0±0.8	8.8±1.3	8.0±1.1	6.3±0.3

Figure 2

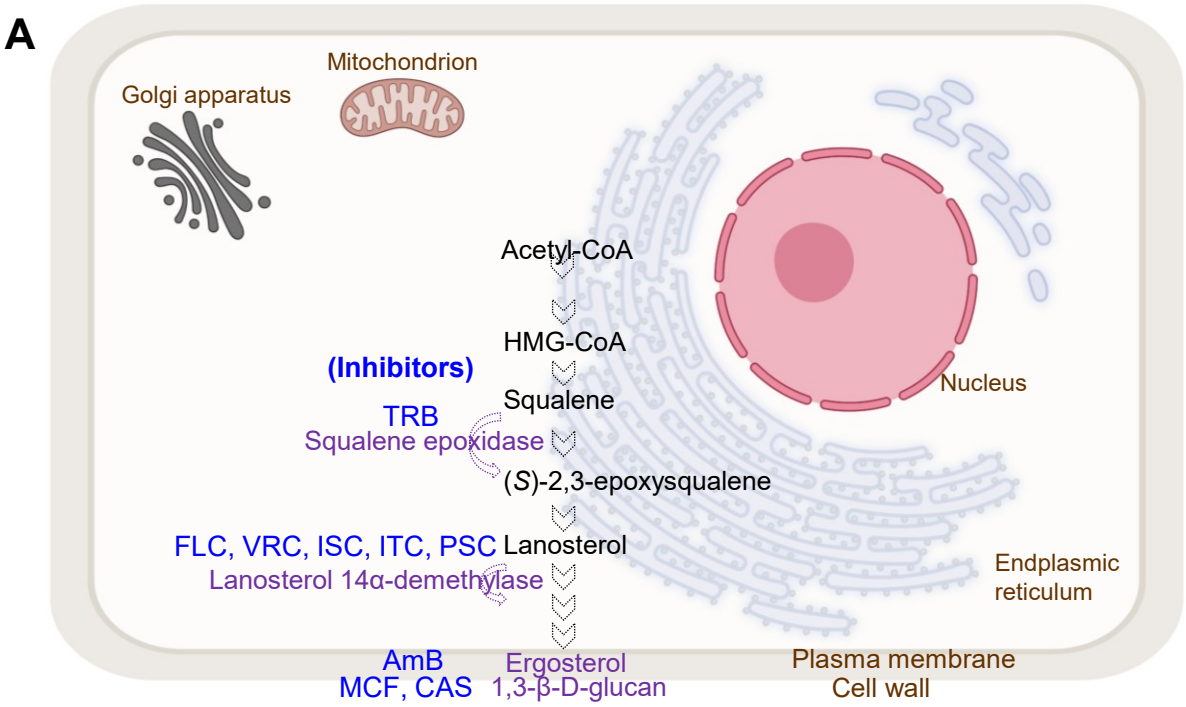

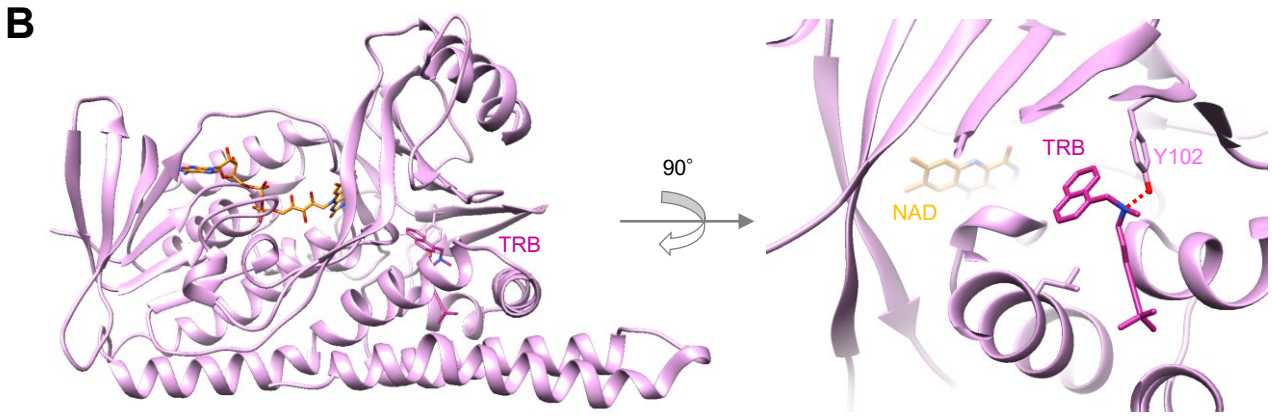

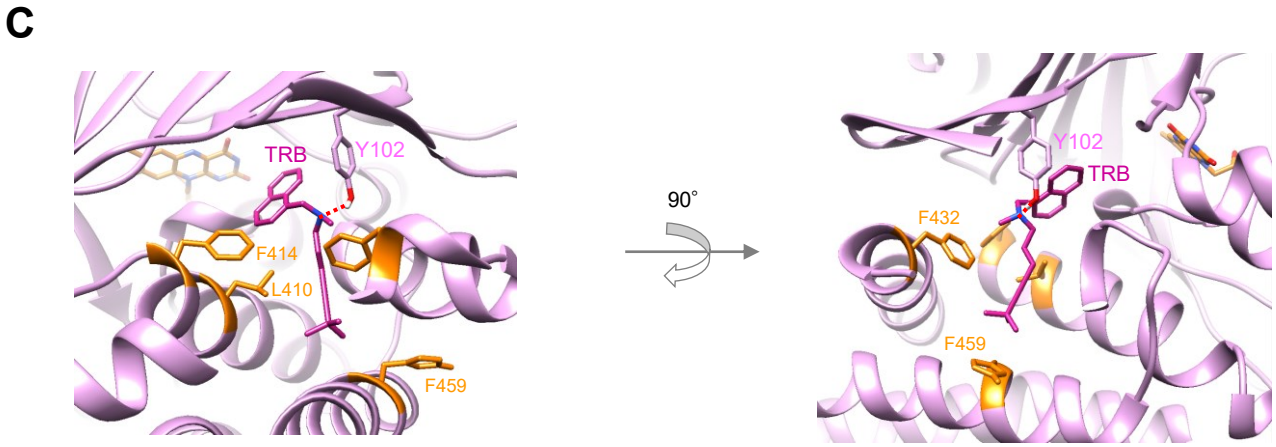

Resistant mutations of TRB in SQLE^{TR}			
L393F/S	F397L	F415L/I/V	H440Y
L410	F414	F432	H459

Corresponding amino acids in SQLE^{ED}

Figure 3

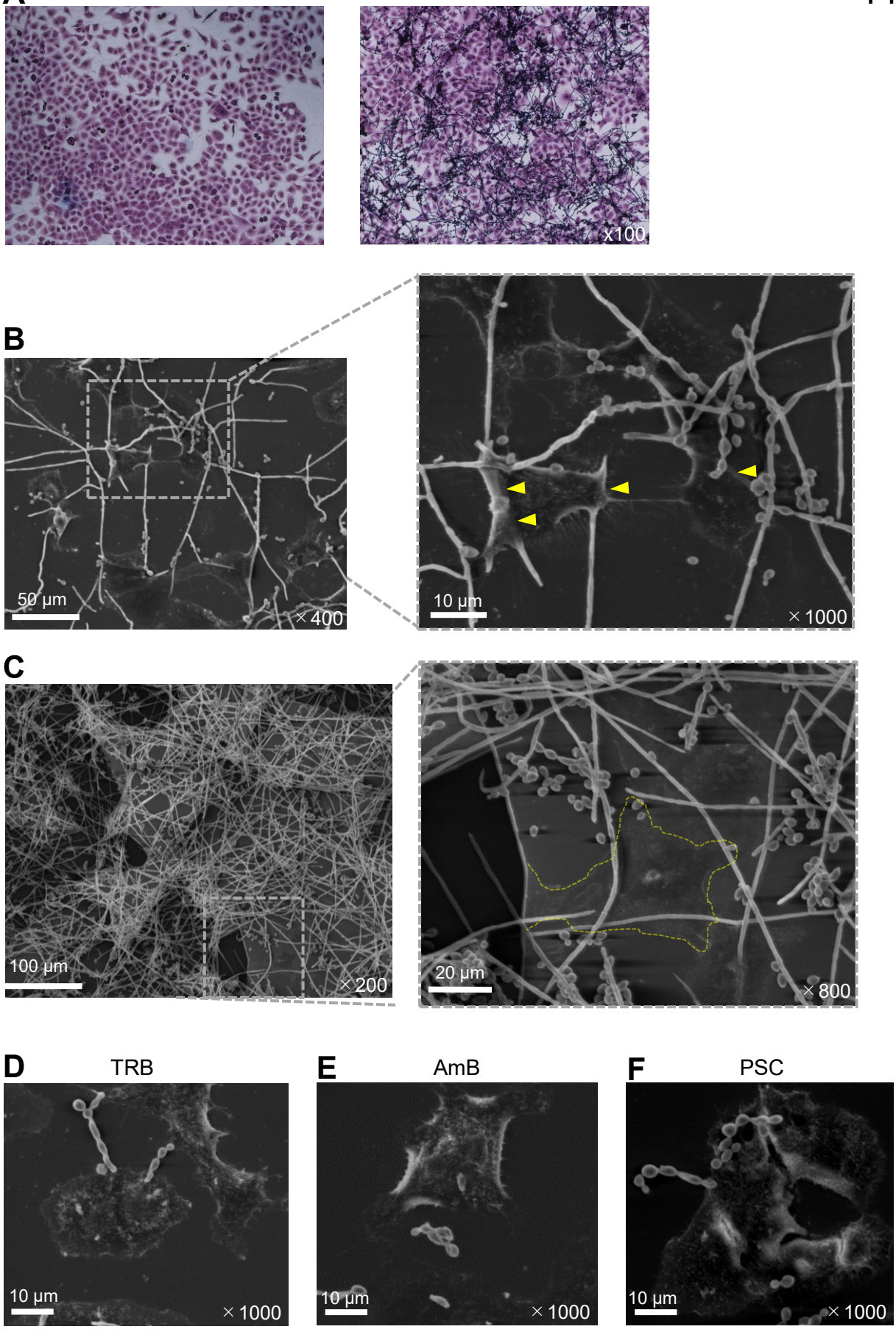
A
x100
B
50 μm
× 400
10 μm
× 1000
C
100 μm
× 200
20 μm
× 800
D
TRB
10 μm
× 1000
E
AmB
10 μm
× 1000
F
PSC
10 μm
× 1000

Figure 4

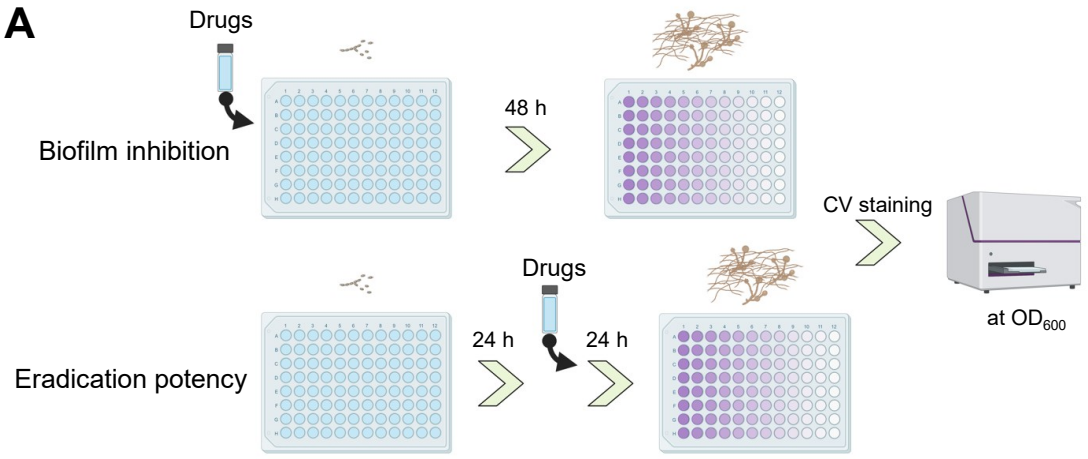
A
Drugs
Biofilm inhibition
48 h
CV staining
at OD600
Drugs
Eradication potency
24 h
24 h

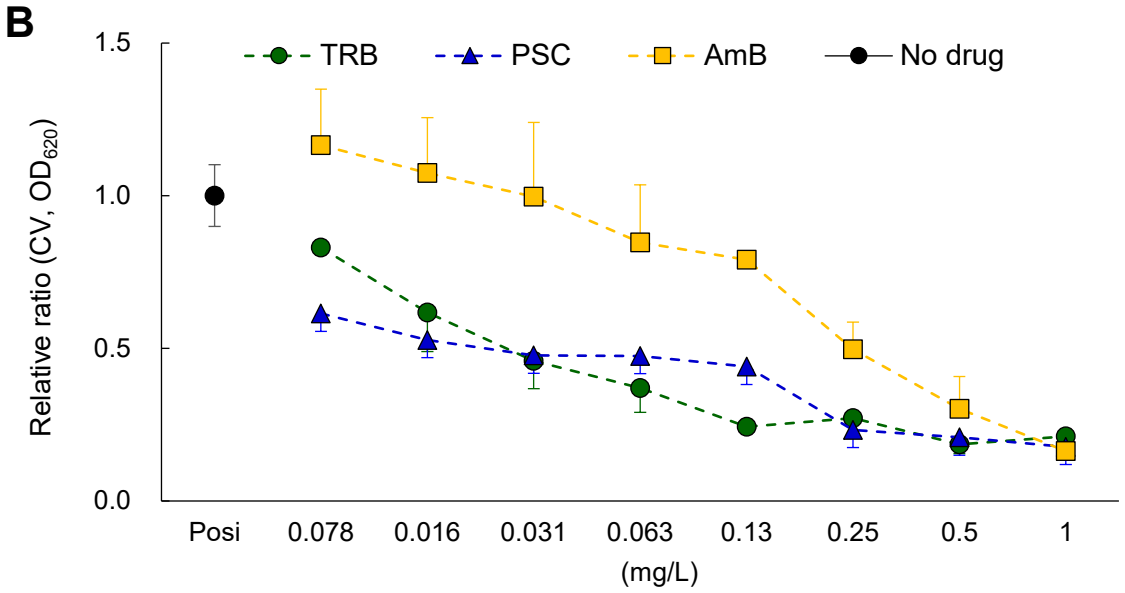
B
TRB
PSC
AmB
No drug
Relative ratio (CV, OD620)
1.5
1.0
0.5
0.0
Posi
0.078
0.016
0.031
0.063
0.13
0.25
0.5
1
(mg/L)

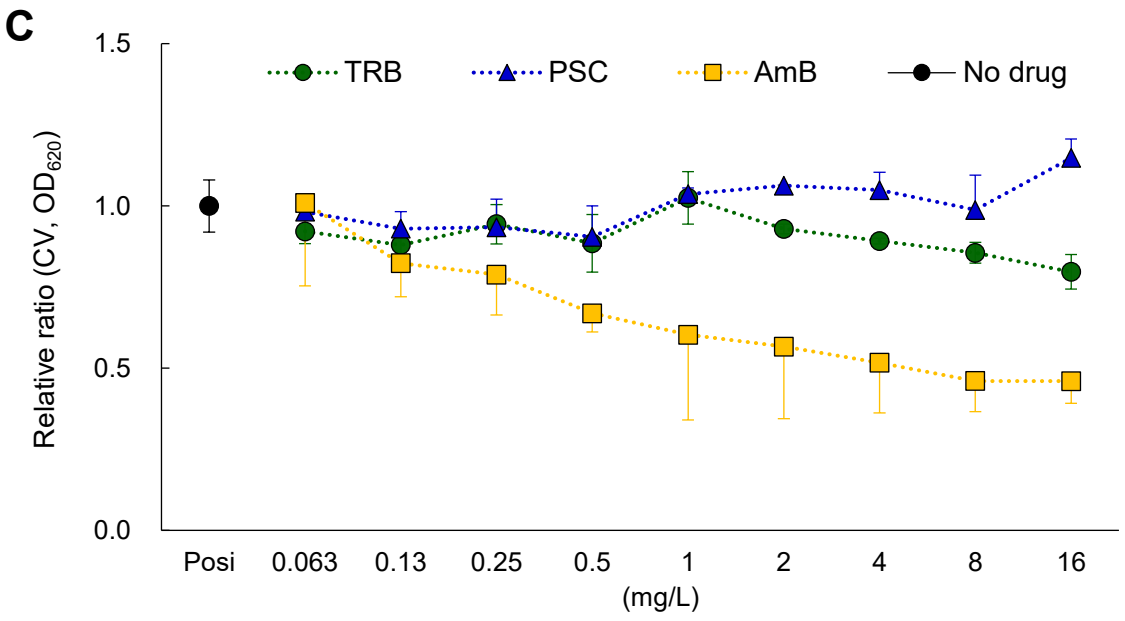
C
TRB
PSC
AmB
No drug
Relative ratio (CV, OD620)
1.5
1.0
0.5
0.0
Posi
0.063
0.13
0.25
0.5
1
2
4
8
16
(mg/L)

Figure 5

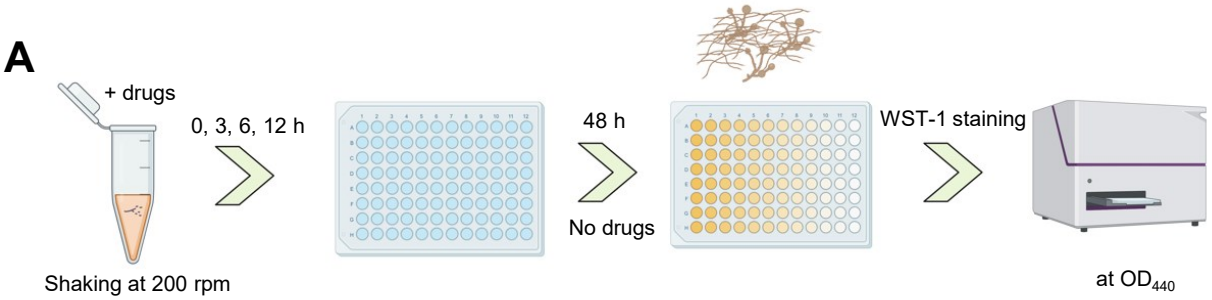
A
+ drugs
0, 3, 6, 12 h
Shaking at 200 rpm
48 h
No drugs
WST-1 staining
at OD440

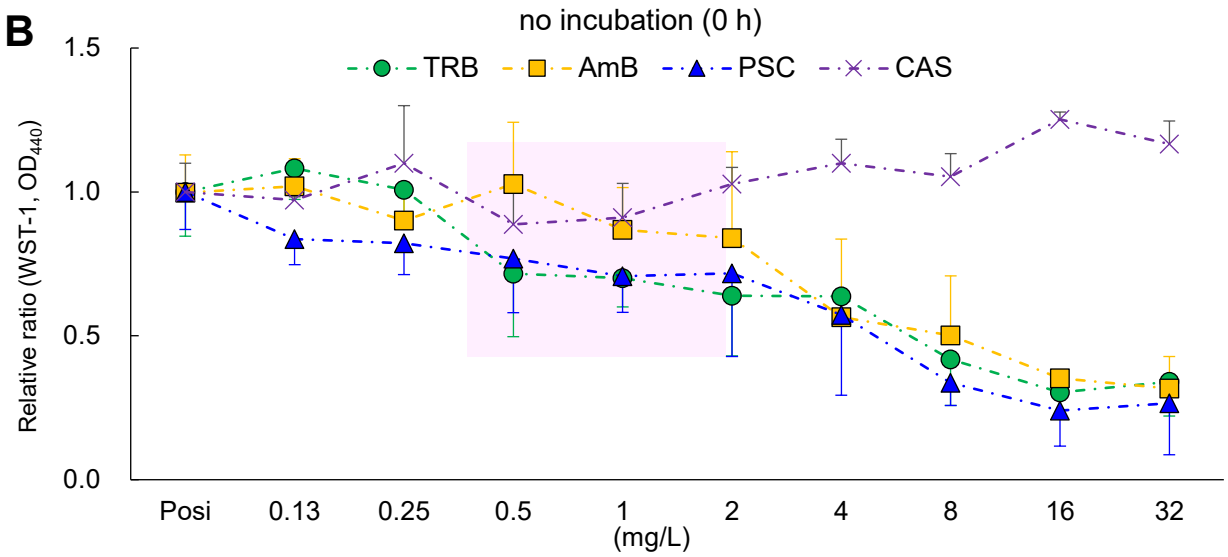
B
no incubation (0 h)
TRB
AmB
PSC
CAS
Relative ratio (WST-1, OD440)
1.5
1.0
0.5
0.0
Posi
0.13
0.25
0.5
1
2
4
8
16
32
(mg/L)

Figure 5

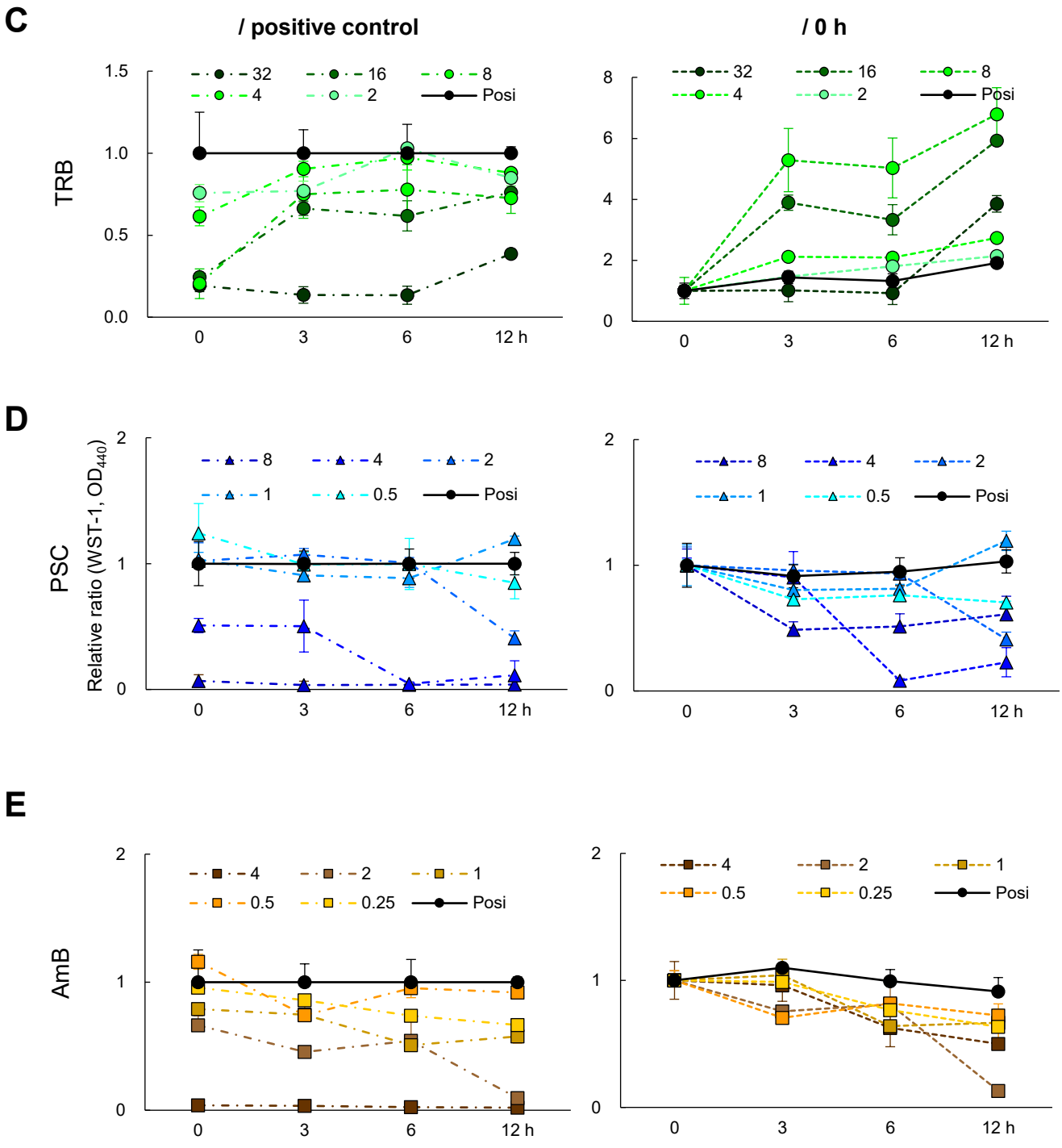
C
/ positive control
/ 0 h
TRB
32
16
8
4
2
Posi
0
3
6
12 h
D
PSC
Relative ratio (WST-1, OD440)
1
0.5
E
AmB
0.25

Figure.6

A

TRB + PSC

Drugs		TRB								
	Conc.	0.5	0.25	0.13	0.063	0.031	0.016	0.0078	0.0039	0
PSC	0.25	0.03	0.03	0.03	0.04	0.03	0.03	0.04	0.04	0.04
	0.13	0.04	0.04	0.03	0.05	0.04	0.03	0.03	0.03	0.05
	0.063	0.03	0.03	0.05	**0.13***	0.37	0.17	0.24	0.21	0.72
	0.031	0.02	0.02	0.06	0.30	0.47	0.22	0.24	**0.44*****	0.76
	0.016	0.02	0.02	**0.02****	0.34	0.49	0.63	0.58	0.61	0.84
	0	0.01	0.00	0.13	0.28	0.55	0.50	0.61	0.55	0.80

0 - 0.1 | 0.1 - 0.5 | 0.5 -

	PSC	TRB	FICI
MIC*	0.5	0.25	**0.75**
MIC_{90} WST-1**	0.5	0.13	**0.63**
MIC_{50} WST-1***	0.25	0.06	**0.31**

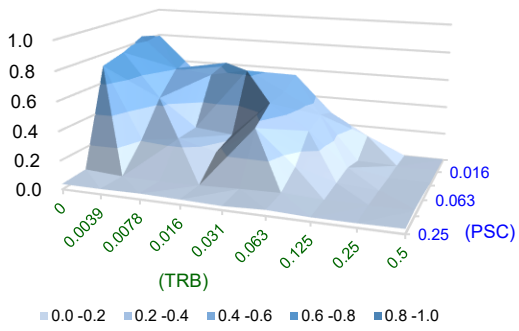

B

TRB + AmB

Drugs		TRB								
	Conc.	0.5	0.25	0.13	0.063	0.031	0.016	0.0078	0.0039	0
AmB	0.5	0.02	0.02	0.01	0.01	0.02	0.01	0.01	0.01	0.01
	0.25	0.02	**0.02****	0.02	0.01	0.02	0.05	0.01	0.01	0.01
	0.13	0.02	0.02	**0.12*/*****	0.17	0.14	0.17	0.12	0.21	0.26
	0.063	0.03	0.03	0.39	0.75	0.68	0.52	0.78	0.50	0.76
	0.031	0.02	0.02	0.37	0.74	0.70	0.75	0.70	0.87	0.82
	0	0.01	0.01	0.23	0.57	0.70	0.89	0.95	1.02	0.87

0 - 0.1 | 0.1 - 0.5 | 0.5 -

	AmB	TRB	FICI
MIC*	0.5	0.5	**1.0**
MIC_{90} WST-1**	1.0	1.0	**2.0**
MIC_{50} WST-1***	1.0	1.0	**2.0**

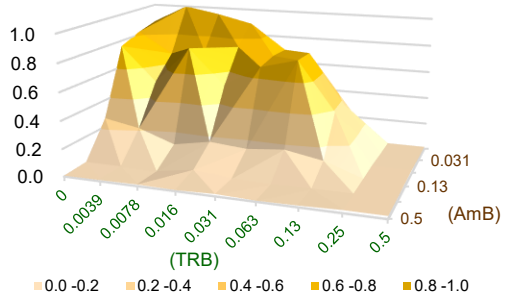

C

AmB + PSC

Drugs		AmB								
	Conc.	0.5	0.25	0.13	0.063	0.031	0.016	0.0078	0.0039	0
PSC	0.25	0.03	0.01	0.02	0.03	0.02	0.04	0.04	0.02	0.01
	0.13	0.07	0.06	0.07	0.05	0.09	**0.02*****	0.05	0.01	0.25
	0.063	0.02	0.03	**0.06****	**0.11***	0.37	0.55	0.14	0.20	0.47
	0.031	0.02	0.02	0.08	0.38	0.71	0.51	0.57	0.51	0.84
	0.016	0.03	0.03	0.09	0.34	0.90	0.73	0.69	0.60	0.93
	0	0.02	0.01	0.02	0.23	0.50	0.62	0.74	0.78	0.78

0 - 0.1 | 0.1 - 0.5 | 0.5 -

	PSC	AmB	FICI
MIC*	0.5	0.5	**1.0**
MIC_{90} WST-1**	1.0	0.5	**1.5**
MIC_{50} WST-1***	0.25	2.0	**2.25**